Comparative Theoretical Study of Adsorption and Dehydrogenation of Formic Acid, Hydrazine and Isopropanol on Pd(111) Surface

Shaodong Zhou · Chao Qian · Xinzhi Chen

Abstract Adsorption and dehydrogenation of formic acid, hydrazine and isopropanol have been investigated using periodic density functional theory (DFT). All the intermediates and transition states have been optimized and the preferred reaction pathways have been found. The adsorption energies for the most stable mode of formic acid, hydrazine and isopropanol are 38.6 kJ/mol, 63.9 kJ/mol and 46.1 kJ/mol, respectively. The dehydrogenation mechanisms of formic acid, hydrazine and isopropanol on Pd(111) surface are proposed and calculated. According to the calculation results, dehydrogenation of formate is more favorable than those of other molecules/groups, and that can be an explanation for the high reactivity of formats in Pd catalyzed transfer hydrogenation.

Keywords Adsorption · Dehydrogenation · DFT study

1 Introduction

Catalytic transfer hydrogenation (CTH) is a practical alternative milder reduction method, which has been used for facile reduction of nitro-compounds and azides to amines, dehalogenation of mono- and poly-chlorinated aryl compounds [1, 2]. Several compounds, such as formic acid (or formate), hydrazine and isopropanol, have been selected as hydrogen donors [3–7], and Pd is a commonly used catalyst. All the experiments indicated that in Pd catalyzed CTH, formic acid and hydrazine were both effective

S. Zhou · C. Qian · X. Chen (✉)
State Key Laboratory of Chemical Engineering (Zhejiang University), Department of Chemical and Biological Engineering, Zhejiang University, Hangzhou 310027, China
e-mail: chemtec@163.com

hydrogen donors, while isopropanol was less active. According to the previous experimental study on CTH [1, 7–9], dehydrogenation of hydrogen donor on Pd surface was a vital process. Though previous reports on CTH experiment revealed macroscopic behavior of the hydrogen donors, the reaction detail remains unknown.

Numerous theoretical and experimental works on the interaction between organic molecules and Pd have been reported. These works mostly focused on the adsorption and dissociation of organic molecules, especially small molecules, on Pd. Periodic slab models and the cluster models have been used in the theoretical studies. If one needs to get insight into dehydrogenation on Pd surface, then periodic slab model is necessary [10]. In this work, Pd(111) model is used to perform comparative investigation on the adsorption and dehydrogenation of different hydrogen donors. Three hydrogen donors, formic acid, hydrazine and isopropanol, will be investigated.

2 Computational Methods

DFT calculations were performed with the program package CASTEP in Materials Studio of Accelrys Inc [11–13]. Plane wave basis functions with spin polarization and the Perdew, Burke, Erzenhof gradient corrected functional (GGA-PBE) were used [14–17]. The transition state search was performed with the linear and quadratic synchronous transit (LST/QST) complete search [18]. Ultrasoft pseudopotential (USP) was used to perform simulation of core electron [19]. Energy cut-off of 400.0 eV was used to improve computational performance.

Pd(111) surface was modeled using three-layer periodic slab model with a (3×3) super cell including 10 Å vacuum slab, within which the adsorption and dehydrogenation

occurs. The reciprocal space of the (3×3) super cell was sampled with the k-points set of $(3 \times 3 \times 2)$. Larger k-points sets are needed if more accurate energy value wanted. Study in this work focused on the relative results of different systems, so the k-points set of $(3 \times 3 \times 2)$ should be enough. To confirm sufficiency of the selected model (super cell of 3×3, k-points set of $3 \times 3 \times 2$ and 3-layer Pd), we compared three calculated adsorption configurations $HCOOH_{bridge}$, $N_2H_{4bridge}$ and $C_3H_{8}O_{on\ top}$ with those calculated on a larger model, negligible discrepancy was produced. Similar model was used previously in calculations of reactions on metal surface and proved to be effective and convincing [20]. Geometry optimization was performed for all the relevant adsorbates with Pd atoms constrained except the uppermost layer. The convergence tolerances of energy and displacement were 2×10^{-5} eV/atom and 2×10^{-3} Å, respectively, and the SCF tolerance was 2×10^{-6} eV/atom.

The adsorption energies were calculated using the equation
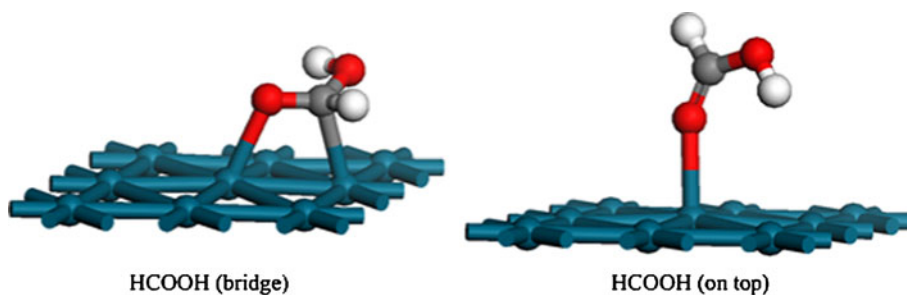
$$E_{ads} = E_{adsorbate-Pd} - E_{adsorbate} - E_{Pd}$$

where E_{ads} represents the adsorption energy of the adsorbate on Pd(111) surface, $E_{adsorbate}$ is the energy of free adsorbate, E_{Pd} is the energy of clean slab and $E_{adsorbate-Pd}$ is the energy of adsorbate-Pd adsorption system.

For a dehydrogenation reaction, which can be represented as: RH → R + H, the energy barrier was calculated as follows:

$$E_a = E_{TS} - E_{RH-Pd}$$

where E_{TS} is the energy of transition state and E_{RH-Pd} is the energy of RH–Pd adsorption system.

3 Results and Discussion

For clarity, this section is organized as follow. First, the adsorption information of formic acid, hydrazine and isopropanol is presented. Then, all the possible reaction pathways for are presented. Finally, the calculation results are summarized.

3.1 Adsorption of Hydrogen Donors on Pd(111)

In this subsection, adsorbed structures and energies for all the involved species are presented. Table 1 tabulates the information of all the possible adsorption modes.

3.1.1 Formic Acid

For free formic acid in gas phase, the calculated bond lengths are 1.106 (1.097) Å for C–H, 1.357 (1.343) Å for C–O1, 1.218 (1.202) Å for C–O2 and 0.986 (0.972) Å for O1–H, our results are in agreement with previous experimental values [21] displayed in the parentheses. Formic acid has two adsorption modes, "on top" and "bridge" (shown in Fig. 1). The calculated adsorption energies are 38.6 kJ/mol and 25.1 kJ/mol for the "bridge" and "on top" mode, respectively. The "bridge" mode forms via cleavage of the carbonyl π bond and bonding between the C, O2 atoms and two neighbor Pd atoms on the surface. The C–Pd, O2–Pd distance are 2.162 Å and 2.185 Å, and the C–O2–Pd, O2–C–Pd, O2–C–H, O2–C–O1 angles are 113.5°, 104.1°, 121.9° and 121.0°, respectively. The four atoms (H, O1, O2 and Pd) that bond with C in formic acid compose a tetrahedron, with C as center. The extension of

Table 1 Adsorption sites, adsorption energies (in kJ/mol), and structural parameters (in angstroms and degrees) for formic acid, HCOO, hydrazine and isopropanol

Species	Sites	E_{ad}	d_{C-Pd}	d_{O-Pd}	d_{N-Pd}
HCOOH	on top	25.1		2.305	
	bridge	38.6	2.162	2.185	
HCOO	on top	37.4		2.011	
	[1]bridge	52.2		2.151, 2.200	
	[3]bridge	58.1		2.121, 2.123	
	fcc	65.1		2.235, 2.318, 2.282	
cis-N$_2$H$_4$	on top	41.8			2.115
	bridge	63.9			2.154, 2.155
anti-N$_2$H$_4$	on top	42.7			2.114
(CH$_3$)$_2$CHOH	on top	46.1		2.212	

fcc face-centered cubic

Fig. 1 View of the adsorption structure of formic acid on Pd (111) surface. *Green ball* represents Pd atom, *white ball* represents H atom, *red ball* represents O atom and *grey ball* represents C atom

HCOOH (bridge)　　　HCOOH (on top)

O2–Pd distance and configuration change of formic acid indicate that the hybridization of C has varied from *sp2* in free formic acid to *sp3* in adsorbed formic acid. This thus proves the cleavage of carbonyl π bond in formic acid. For "on top" mode, formic acid is adsorbed via the single O–Pd bond. The O–Pd distance is 2.305 Å, the C–O–Pd and O′–O–Pd angles are 156.5° and 129.2°, respectively. The molecule-surface distance in "on top" mode is about 0.2 Å longer than that in "bridge" mode, consist with the lower adsorption energy of "on top" mode. The calculation result indicates that the "on top" mode has a much lower adsorption energy on Pd(111) surface. Previous study gave less discrepancy on adsorption energies for the two adsorption modes on Pd(100) surface [22], probably due to the different Pd atom distributions on Pd(111) and Pd(100) surface.

3.1.2 Hydrazine

For *gauche*-hydrazine in gas phase, the calculated bond lengths and angles are 1.024 (1.015) Å for N–H, 1.447 (1.447) Å for N1–N2, 112.0°(112°) for N1–N2–H1 angle and 108.3°(106°) for N1–N2–H2 angle, consistent with previous experimental data [23]. For *anti*-hydrazine in gas phase, the calculated bond lengths and angles are 1.491 Å for N1–N2, 1.034 Å for N1–H, 104.1° for N1–N2–H1 angle and 104.0° for N1–N2–H2 angle. Hydrazine can be adsorbed via three modes, "bridge" for *cis*-hydrazine, "on top" for *gauche*- and *anti*-hydrazine (shown in Fig. 2). For the adsorption mode *cis*-hydrazine$_{bridge}$, the bond lengths of N1–N2, N1–Pd and N2–Pd are 1.461 Å,

1.154 Å, 1.155 Å, respectively, and the angles of N1–N2–Pd and N2–N1–Pd are 105.6° and 108.4°. *gauche*-Hydrazine and *anti*-hydrazine have similar adsorption configurations of "on top" mode, the N–Pd bond lengths are 2.115 and 2.114, and the N2–N1–Pd angles are 117.3° and 121.8°, respectively. The calculation results indicate that the adsorption energy for "bridge" mode of *cis*-hydrazine is 63.9 kJ/mol, much more than that for "on top" mode of *cis*-hydrazine (41.8 kJ/mol) and *anti*-hydrazine (42.7 kJ/mol). The distance between hydrazine molecule and Pd surface is about 2.05 Å for "bridge" adsorption mode, while the distances are about 2.10 Å for the other two "on top" modes. Thus the shorter distance between hydrazine and Pd surface for "bridge" mode is in accord with the higher binding energy.

In acidic environment, hydrazine exists mainly as $N_2H_6^{2+}$, in which the N atoms donate the lone-pair electrons to bond with proton. Taking account of the steric hindrance around N atoms, $N_2H_6^{2+}$ may have a weak adsorption mode, and it is proved by the calculated weak adsorption energy (9.2 kJ/mol). We have also compared the density of states (DOS) of "naked" $N_2H_6^{2+}$, Pd slab and $N_2H_6^{2+}$/Pd. It is clear in Fig. 3 that no peak of new bonds appeared in adsorbed $N_2H_6^{2+}$–Pd system. The small peaks between 15 and 25 eV could be attributed to the inductive effect of Pd surface to the $N_2H_6^{2+}$ group. So $N_2H_6^{2+}$ binds onto Pd surface via physisorption. Then it is also difficult for $N_2H_6^{2+}$ to be dehydrogenated on Pd surface. Then we can conclude that basic environment favors the CTH that using hydrazine as hydrogen donor, consistent with previous experiment [7].

Fig. 2 View of the adsorption structure of hydrazine on Pd (111) surface. Notation of atom is as same as Fig. 1, and *blue ball* represents N atom
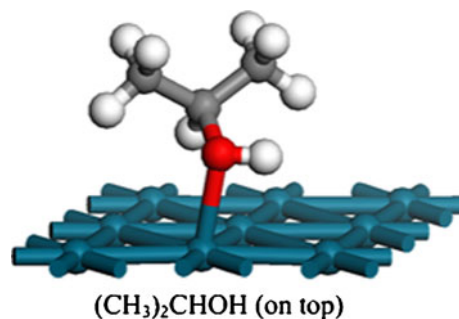
cis-N$_2$H$_4$ (bridge)   *gauche*-N$_2$H$_4$ (on top)

anti-N$_2$H$_4$ (on top)
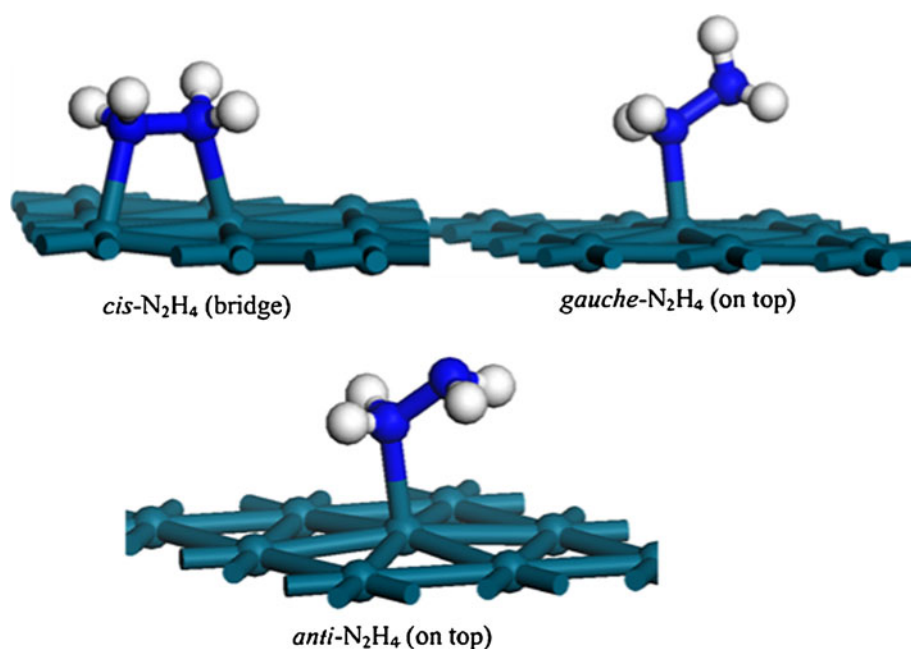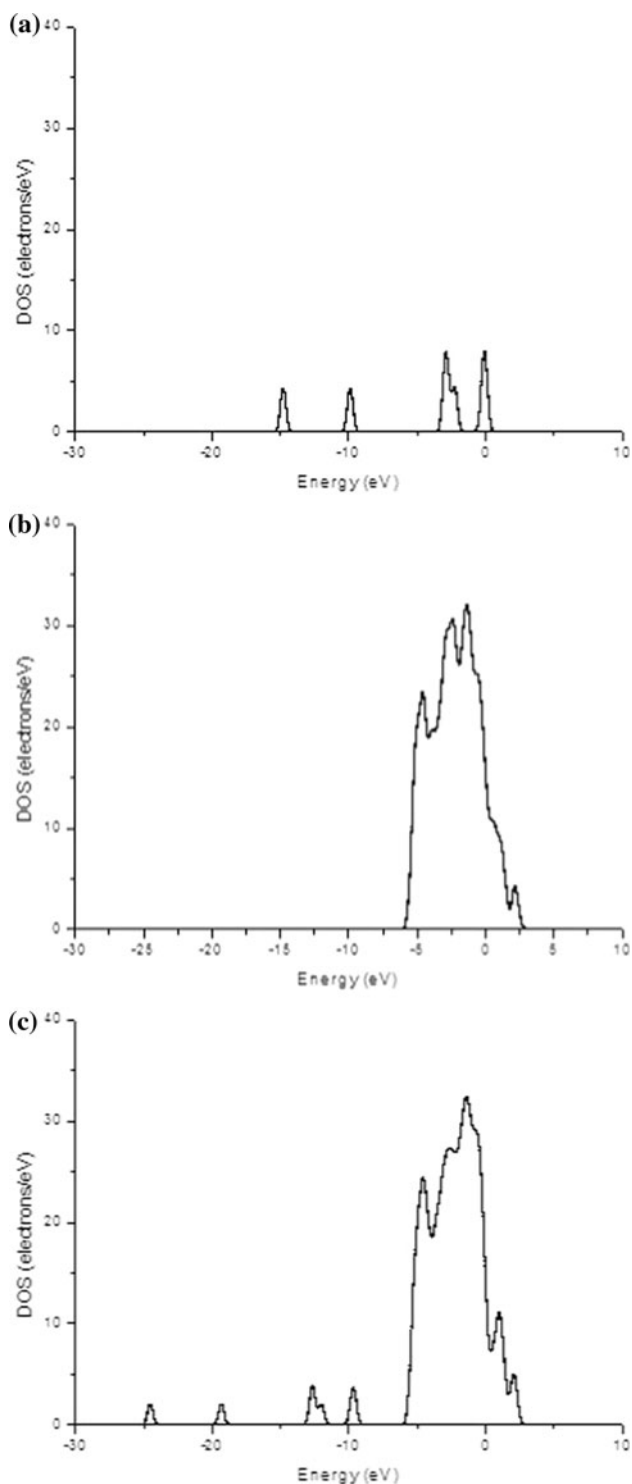
Fig. 3 Density of states (DOS) of (a) "naked" N2H4, (b) Pd(111) surface and (c) adsorbed N2H6 on Pd(111) surface

3.1.3 Isopropanol

For isopropanol in gas phase, the calculated bond lengths and angles are 1.448 (1.431) Å for C1–O, 0.976 (0.97) Å for O–H, 112.7°(112°) for C2–C1–C3 and 108.1°(105°) for

Fig. 4 View of the adsorption structure of isopropanol on Pd (111) surface. Notation of atom is as same as Fig. 1

C1–O–H, respectively, consistent with the calculated results [24]. It is generally believed that isopropanol is adsorbed via donation of the lone-pair electrons of O atom to solid surfaces [25, 26] (shown in Fig. 4), which is exhibited as "on top" mode. For isopropanol adsorbed via "on top" mode, the bond lengths of C–O, O–H and O–Pd are 1.487 Å, 0.981 Å and 2.212 Å, the angles C–O–H and C–O–Pd are 107.5° and 119.2°, respectively. The adsorption energy is 46.1 kJ/mol.

3.2 Dehydrogenation of Hydrogen Donors on Pd(111)

In this section, possible dehydrogenation pathways of the three species will be presented. Reaction energy and barrier of every elementary reaction are shown in Table 2.

3.2.1 Dehydrogenation of Formic Acid

Dehydrogenation of formic acid involves several pathways, which initiated by cleavage of C–H bond or O–H bond for both of the two adsorption modes. We performed calculation of the possible dehydrogenation routes, and the preferred pathway is shown in Fig. 5.

3.2.1.1 Initial O–H Bond Cleavage for "bridge" Mode Three reaction pathways are involved into the dehydrogenation for "bridge" mode initialized by cleavage of O–H bond. In the initial step, the O–H bond is ruptured and Pd–H bond forms. Then the rest group rotates to form "on top" adsorption mode. However, HCOO has three more stable adsorption modes, "^{1}bridge", "^{3}bridge" and "fcc" (see Fig. 6). The adsorption geometries and energies of HCOO are shown in Table 1. Zhang et al. [27] reported experimental parameters of adsorbed HCOO via "^{3}bridge" mode, the detected bond lengths of O–Pd and C–O are 2.16 ± 0.06 Å (calculated values: 2.121 Å and 2.123 Å) and 1.26 ± 0.05 Å (calculated values: 1.274 Å and 1.274 Å), respectively, and the O–C–O angle is 130 ± 5° (calculated values: 129.6°). Thus our calculation results are in good agreement with the previous experiment. The "on

Table 2 Calculated reaction energies ΔE and energy barriers E_a (in kJ/mol) for all the elementary reactions

Reactions	ΔE	E_a
$HCOOH_{bridge} \rightarrow HCOO_{on\ top} + H$	11.2	20.2
$HCOO_{on\ top} \rightarrow CO_2 + H$	−23.5	38.5
$HCOO_{on\ top} \rightarrow HCOO_{1bridge}$	−14.7	0.5
$HCOO_{1bridge} \rightarrow CO_2 + H$	−9.3	16.5
$HCOO_{on\ top} \rightarrow HCOO_{3bridge}$	−26.7	15.7
$HCOO_{3bridge} \rightarrow CO_2 + H$	3.1	49.2
$HCOO_{on\ top} \rightarrow HCOO_{fcc}$	−17.9	0
$HCOO_{fcc} \rightarrow CO_2 + H$	−15.9	50.0
$HCOO_{fcc} \rightarrow HCOO_{1bridge}$	3.1	5.8
$HCOO_{fcc} \rightarrow HCOO_{3bridge}$	−8.8	18.5
$HCOOH_{on\ top} \rightarrow HCOO_{on\ top} + H$	8.4	12.5
$HCOOH_{on\ top} \rightarrow COOH_{on\ top} + H$	−10.5	26.8
$HCOOH_{bridge} \rightarrow H + COOH_{bridge}$	−14.4	21.0
$COOH_{bridge} \rightarrow CO_2 + H$	−9.5	25.4
$COOH_{bridge} \rightarrow CO + OH_{bridge}$	−1.7	20.7
$OH_{bridge} \rightarrow O + H$	−8.0	56.5
$H_2NNH_{2\ bridge} \rightarrow H_2NNH_{bridge} + H$	4.8	31.0
$H_2NNH_{bridge} \rightarrow H + HNNH_{bridge}$	11.6	29.2
$HNNH_{bridge} \rightarrow HNN_{bridge} + H$	2.8	27.9
$HNN_{bridge} \rightarrow N_2 + H$	−30.5	12.0
$H_2NNH_{bridge} \rightarrow H_2NN_{bridge} + H$	−1.9	57.1
$H_2NNH_{2bridge} \rightarrow H_2N + NH_2$	15.6	45.9
$(CH_3)_2CHOH_{on\ top} \rightarrow (CH_3)_2CHO_{on\ top} + H$	16.7	21.2
$(CH_3)_2CHO_{on\ top} \rightarrow (CH_3)_2CO + H$	−25.2	34.4
$(CH_3)_2CHO_{on\ top} \rightarrow (CH_3)_2CHO_{fcc}$	−11.7	9.3
$(CH_3)_2CHO_{fcc} \rightarrow (CH_3)_2CO + H$	−9.0	54.8
$(CH_3)_2CHOH_{on\ top} \rightarrow (CH_3)_2C–OH_{on\ top} + H$	15.7	39.3
$(CH_3)_2C–OH_{on\ top} \rightarrow (CH_3)_2CO + H$	−10.6	22.7

top" mode can be transformed into "fcc" mode easily with no energy barrier, into "^{1}bridge" and "^{3}bridge" modes with barriers of 0.5 kJ/mol and 15.7 kJ/mol, respectively. The "fcc" mode can be transformed into "^{1}bridge" and "^{3}bridge" modes with barriers of 5.8 kJ/mol and 18.5 kJ/mol, respectively. Among the three adsorption modes of HCOO, the "^{1}bridge" mode has the lowest C–H bond cleavage barrier (16.5 kJ/mol).

The cleavage of O–H bond for "bridge" mode is endothermic by 11.2 kJ/mol with a energy barrier of 20.2 kJ/mol, which means that it is a slow step. Our result suggests that the "^{3}bridge" mode for HCOO is the most stable adsorption mode with binding energy of 49.2 kJ/mol, consistent with the experiment [28]. Of all the three adsorption modes of HCOO, "^{1}bridge" has the lowest dehydrogenation barrier. Besides, the mode transformation from "fcc" to "^{1}bridge" is also a fast step (with barrier of 5.8 kJ/mol and reaction energy of 3.1 kJ/mol).

3.2.1.2 Initial C–H Bond Cleavage for "bridge" Mode The cleavage of C–H bond for "bridge" mode is exothermic by 14.4 kJ/mol with energy barrier of 21.0 kJ/mol. After cleavage of C–H bond, a stable adsorption mode of COOH forms. The decomposition of adsorbed COOH may proceed along two pathways, $COOH \rightarrow CO_2 + H$ and $COOH \rightarrow CO + OH$, the calculation result indicates that the latter pathway is preferable. However, the dehydrogenation of OH is thermodynamically unfavorable with a high energy barrier of 56.5 kJ/mol. Taking account of that CO can escape from Pd surface, the decomposition of COOH can hardly produce active H.

3.2.1.3 Initial O–H Bond Cleavage for "on top" Mode Dehydrogenation of formic acid for "on top" adsorption mode on Pd(100) has already been studied by Clarence, Yue and Lim [22]. Their calculation result showed little difference between initial cleavage of O–H bond and C–H bond thermodynamically, so the reaction should proceed along both of the two pathways according to their conclusion. However, our calculation result indicates that for adsorbed HCOOH on Pd(111) surface, the initial O–H bond cleavage is more favorable kinetically by 10.3 kJ/mol. So dehydrogenation of formic acid for "on top" mode is mainly initiated by cleavage of O–H bond. Further discussion will base on this approach.

Cleavage of O–H bond for "on top" mode HCOOH has a barrier of 12.5 kJ/mol and the reaction energy is 8.4 kJ/mol. Then the "on top" adsorption of HCOO forms, subsequent reaction pathways are as same as those discussed in Sect. 3.2.1.1.

*3.2.1.4 Summary of Dehydrogenation of Formic Acid* After comparing all the elementary reactions, we can get the most favorable reaction pathway for dehydrogenation of formic acid on Pd(111) surface. Although the pathway $HCOOH_{on\ top} \rightarrow HCOO_{on\ top} + H \rightarrow HCOO_{1bridge} \rightarrow CO_2 + H$ has the lowest barrier, the "on top" adsorption mode of HCOOH is much less stable than "bridge" mode (by 13.5 kJ/mol). Thus only a few of the HCOOH molecules are adsorbed via "on top" mode, so the dehydrogenation is initiated from the "bridge" mode. Then the preferred pathway for the whole process of dehydrogenation of HCOOH is $HCOOH \rightarrow HCOOH_{bridge} \rightarrow HCOO_{on\ top} + H \rightarrow HCOO_{1bridge} \rightarrow CO_2 + H$. Therefore, almost all the product of dehydrogenation of formic acid is CO_2, consistent with the CTH experiments [1, 4, 6]. Compared to formic acid, formate has more stable adsorption mode, so dehydrogenation of formate is more favorable than that of formic acid. So according to our calculation, formates are more effective hydrogen donors than formic acid, in agreement with the comparative experiment results [1, 2, 29].

Fig. 5 Elementary reactions of preferred pathway for dehydrogenation of formic acid on Pd (111) surface
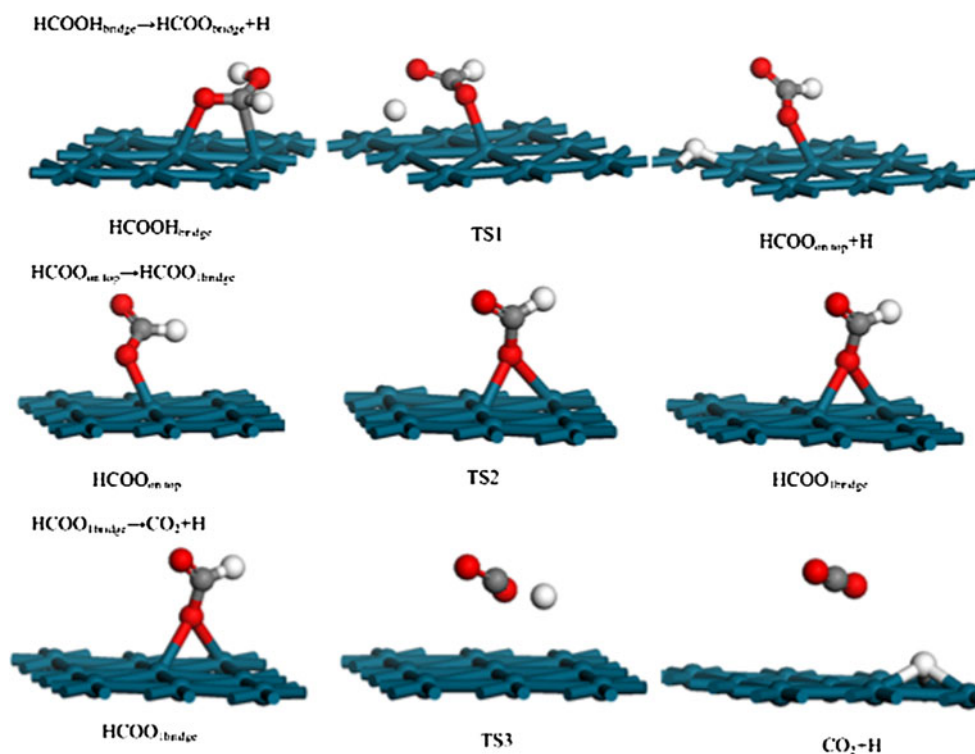
Fig. 6 View of the adsorption structure of HCOO on Pd (111) surface. Notation of atom is as same as Fig. 1
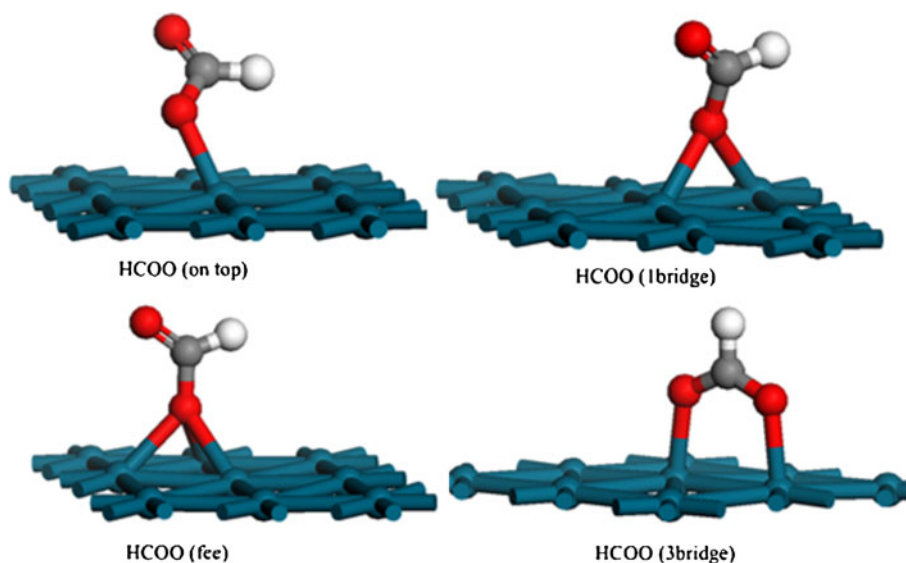
### 3.2.2 Dehydrogenation of Hydrazine

Considering the significant difference on the adsorption energy between the three adsorption modes of hydrazine, almost all the hydrazine adsorbs via "bridge" mode of *cis*-hydrazine, so dehydrogenation of hydrazine will be investigated on the "bridge" model. The calculated structures of the reactants, intermediates and transition states for proposed reaction pathways are shown in Fig. 7.

It is clear in Table 2 that dehydrogenation of hydrazine mainly proceeds as H_2NNH_2 $_{bridge}$ → H_2NNH_{bridge} + H → H + $HNNH_{bridge}$ → HNN_{bridge} + H → N_2 + H. After dissociation of the first two H atom, the H–N–N–H dihedral angle is unfolded so that the last four atoms share a plane which parallels with Pd surface. Dissociations of the first three H have comparable reaction barriers, while the dissociation of the last H atom is much easier due to the instability of N_2H.

We have also tried to perform calculation of dehydrogenation of hydrazine as an alternative sequence, but a high energy barrier (57.1 kJ/mol) has been found for the dissociation H_2NNH → H_2NN + H. So it is very difficult for

Fig. 7 Elementary reactions of preferred pathway for dehydrogenation of hydrazine on Pd (111) surface
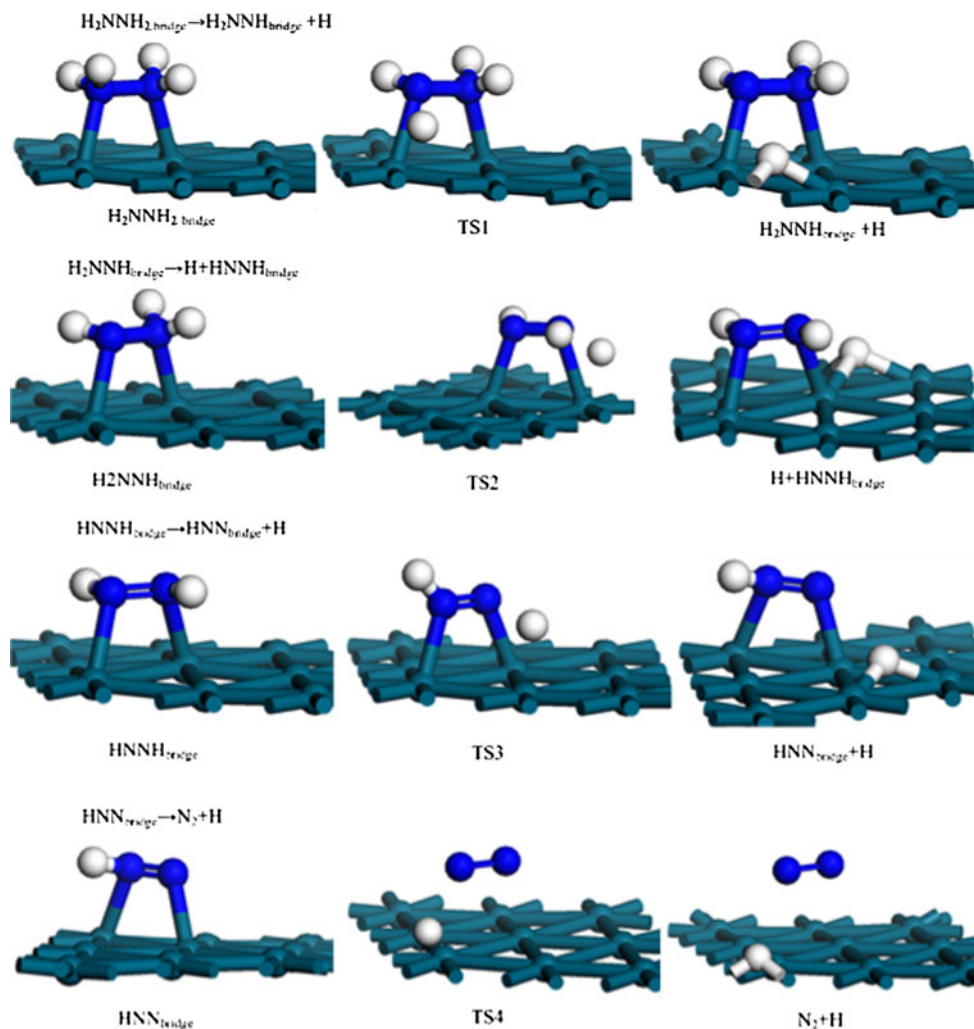
the reaction to proceed along this pathway. We also considered cleavage of the N–N bond, but the high barrier and reaction energy indicated that it cannot lead to a preferred reaction pathway. No ammonia was detected in our experiment carried out in basic solution, consistent with the calculation results.

3.2.3 Dehydrogenation of Isopropanol

Three reaction pathways are found for dehydrogenation of isopropanol, involving four elementary reactions. The calculated structures of the reactants, products, intermediates and transition states for preferred pathways are shown as Fig. 8.

For the first pathway, the initial step is the cleavage of C–H bond on the tertiary carbon. The first step has the highest reaction barrier along the pathway (39.3 kJ/mol). Then new adsorption mode forms via formation of the C-Pd bond (tertiary carbon). The second step is the cleavage of O–H bond, with a barrier of 22.7 kJ/mol.
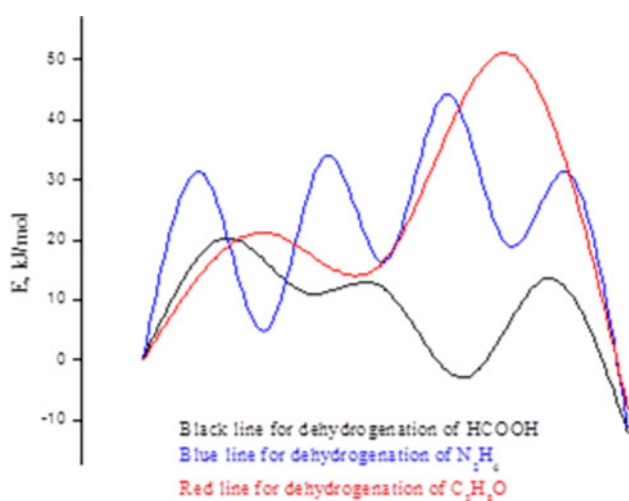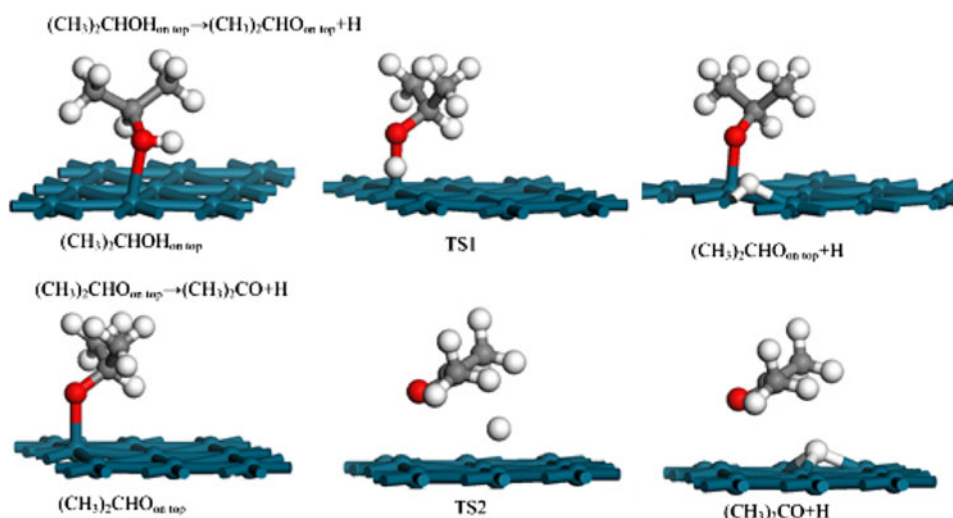
For both of the other two pathways, the first step is the cleavage of O–H bond. This reaction is energy unfavorable by 21.2 kJ/mol. Then the "on top" adsorption mode of C_3H_7O forms, which is less stable and prone to be transformed into "fcc" mode. No stable "bridge" adsorption mode of C_3H_7O has been found. Dehydrogenation of C_3H_7O for "on top" mode has lower energy barrier than that the "fcc" mode and it is thermodynamically favorable. Dehydrogenation for "fcc" mode is a slow step with a high barrier of 54.8 kJ/mol.

Thus the possible reaction pathways of dehydrogenation of isopropanol have been found, the reaction prefers cleavage of O–H bond initially, following by subsequent cleavage of C–H bond from "on top" mode.

3.2.4 Summary of Dehydrogenation

From Table 2 we can see that in all the preferred pathways, dehydrogenation of formic acid has the lowest energy barrier (16.5 kJ/mol). So dehydrogenation of formic acid is

Fig. 8 Elementary reactions of preferred pathway for dehydrogenation of isopropanol on Pd (111) surface

$(CH_3)_2CHOH_{on\ top} \rightarrow (CH_3)_2CHO_{on\ top} + H$

$(CH_3)_2CHOH_{on\ top}$ TS1 $(CH_3)_2CHO_{on\ top} + H$

$(CH_3)_2CHO_{on\ top} \rightarrow (CH_3)_2CO + H$

$(CH_3)_2CHO_{on\ top}$ TS2 $(CH_3)_2CO + H$

Fig. 9 Energy profiles of preferred reaction pathways for dehydrogenation of formic acid, hydrazine and isopropanol

Black line for dehydrogenation of HCOOH
Blue line for dehydrogenation of N_2H_4
Red line for dehydrogenation of C_3H_8O

much easier to proceed than the other two species both kinetically. The energy profiles of the preferred reaction pathways are shown in Fig. 9. It is notable that HCOO can be adsorbed more stably than formic acid, so formaets should be the most effective hydrogen donor in Pd catalyzed CTH. As dehydrogenation of isopropanol has a higher energy barrier and lower adsorption energy than hydrazine, isopropanol should be less reactive in Pd catalyzed CTH. Previous experimental study has given a good proof for this approach [7].

4 Conclusions

Adsorption and dehydrogenation of formic acid, hydrazine and isopropanol have been investigated using DFT. We have summarized the main points of this work as follows.

(1) Formic acid adsorbs on Pd(111) surface via two modes, "on top" and "bridge". Of all the species, hydrazine has the highest adsorption energy ("bridge" mode). There is only one stable adsorption mode for isopropanol, "on top" mode.

(2) $N_2H_6^{2+}$ is found difficult to be adsorbed on Pd(111) surface. So basic condition is favorable for Pd catalyzed CTH reactions that use hydrazine as hydrogen donor.

(3) All the preferred pathways for dehydrogenation of the three species are obtained. For formic acid, the most favorable reaction pathway is $HCOOH_{bridge} \rightarrow HCOO_{on\ top} + H \rightarrow HCOO_{1bridge} \rightarrow CO_2 + H$, for hydrazine is $H_2NNH_2 \rightarrow H_2NNH + H \rightarrow HNNH + H \rightarrow HNN + H \rightarrow N_2 + H$, for isopropanol is $C_3H_7OH_{on\ top} \rightarrow C_3H_7O_{on\ top} + H \rightarrow C_3H_6O + H$.

(4) The preferred pathway for dehydrogenation of formic acid is found to be much more favorable than that of hydrazine and isopropanol, and hydrazine is more effective as hydrogen donor than isopropanol. Furthermore, as HCOO has more stable adsorption mode than formic acid, we can also explain why formate is more effective in Pd catalyzed CTH.

In order to get further insight into Pd catalyzed CTH reaction, the hydrogenation of acceptors should be introduced into the calculations, and a lot of work need to be done.

References

1. Rajagopal S, Spatola AF (1995) J Org Chem 60:1347
2. Arcadi A, Gerichelli G, Chiarini M, Vico R, Zorzan D (2004) Eur J Org Chem 2004:3404

3. Cellier PP, Spindler JF, Taillefer M et al (2003) Tetrahedron Lett 44:7191
4. Ukisu Y (2008) Appl Catal A: Gen 349:229
5. Sydnes MO, Isobe M (2008) Tetrahedron Lett 49:1199
6. Wiener H, Blum J, Sasson Y (1991) J Org Chem 56:4481
7. Kopinke FD, Machenzie K, Koehler R, Georgi A (2004) Appl Catal A: Gen 271:119
8. Reddy PG, Baskaran S (2002) Tetrahedron Lett 43:1919
9. Tike MA, Mahajani VV (2006) Chem Eng J 123:31
10. German ED, Sheintuch M (2008) J Phys Chem C 112:14377
11. Srivastava GP, Weaire D (1987) Adv Phys 26:463
12. Marlo M, Milman V (2000) Phys Rev B 62:2899
13. Payne MC, Teter MP, Allan DC, Arias TA, Joannopoulos JD (1992) Rev Mod Phys 64:1045
14. Delley B (2000) J Chem Phys 113:7756
15. Gajdos M, Eichler A, Hafner J (2004) J Phys: Condens Matter 16:1141
16. Van Santen RA, Neurock M (1995) Catal Rev Sci Eng 37:557
17. Gil A, Clotet A, Ricart MJ, Kresse G, Garcia-Hernandez M, Roesch N, Sautet P (2003) Surf Sci 530:71
18. Perdew JP, Burke K, Ernzerhof M (1996) Phys Rev Lett 77:3865
19. Halgren TA, Lipscomb WN (1977) Chem Phys Lett 49:225
20. Vanderbilt D (1990) Phys Rev B 41:7892
21. Staykov A, Kamachi T, Ishihara T, Yoshizawa K (2008) J Phys Chem C 112:19501
22. Landolt-Boernstein (1976) Structure data of free polyatomic molecules, vol II/7., New SeriesSpringer, Berlin
23. Yue C, Lim KH (2009) Catal Lett 128:221
24. Tarmyshov KB, Mvller-Plathe F (2007) J Chem Phys 126:074702
25. Harcourt RD, Klapoetke TM, White PS (1998) Inorg Chim Acta 269:1
26. Feng G, Huo CF, Deng CM, Huang L, Li YW, Wang JG, Jiao HJ (2009) J Mol Catal A: Chem 304:58
27. Zheng T, Stacchiola D, Saldin DK, James J, Sholl DS, Tysoe WT (2005) Surf Sci 574:166
28. Rajagopal S, Spatola AF (1997) Appl Catal A: Gen 152:69
29. Cai S, Sohlberg K (2003) J Mol Catal A: Chem 193:157